AGU PUBLICATIONS

Geophysical Research Letters

RESEARCH LETTER
10.1002/2014GL062769

**Key Points:**
- Southern Ocean mean calcification rate has declined but trends are heterogeneous
- Trends in particulate inorganic carbon drive calcification trends
- Decreases in carbonate ion are concurrent with decreases in calcification

**Supporting Information:**
- Figure S1–S5
- Table S1

**Correspondence to:**
N. M. Freeman,
natalie.freeman@colorado.edu

**Citation:**
Freeman, N. M., and N. S. Lovenduski (2015), Decreased calcification in the Southern Ocean over the satellite record, *Geophys. Res. Lett.*, *42*, 1834–1840, doi:10.1002/2014GL062769.

Received 5 DEC 2014
Accepted 18 FEB 2015
Accepted article online 23 FEB 2015
Published online 19 MAR 2015

# Decreased calcification in the Southern Ocean over the satellite record

**Natalie M. Freeman[1] and Nicole S. Lovenduski[1]**

[1]Department of Atmospheric and Oceanic Sciences and Institute of Arctic and Alpine Research, University of Colorado Boulder, Boulder, Colorado, USA

**Abstract** Widespread ocean acidification is occurring as the ocean absorbs anthropogenic carbon dioxide from the atmosphere, threatening marine ecosystems, particularly the calcifying plankton that provide the base of the marine food chain and play a key role within the global carbon cycle. We use satellite estimates of particulate inorganic carbon (PIC), surface chlorophyll, and sea surface temperature to provide a first estimate of changing calcification rates throughout the Southern Ocean. From 1998 to 2014 we observe a 4% basin-wide reduction in summer calcification, with ~9% reductions in large regions ($\sim 1 \times 10^6$ km$^2$) of the Pacific and Indian sectors. Southern Ocean trends are spatially heterogeneous and primarily driven by changes in PIC concentration (suspended calcite), which has declined by ~24% in these regions. The observed decline in Southern Ocean calcification and PIC is suggestive of large-scale changes in the carbon cycle and provides insight into organism vulnerability in a changing environment.

## 1. Introduction

The dissolution of carbon dioxide ($CO_2$) in seawater alters carbonate chemistry by lowering pH and reducing the carbonate ion concentration $\left[CO_3^{2-}\right]$. A reduction in $\left[CO_3^{2-}\right]$ lowers the saturation state of seawater with respect to calcite and aragonite, the two forms of mineral calcium carbonate ($CaCO_3$). Coccolithophores are calcifying phytoplankton that play a key role in the biological pump; they secrete calcite shells that act as ballast, helping to export carbon from the surface to the deep. As more of the water column becomes undersaturated in the future [*Fabry et al.*, 2009], dissolution of $CaCO_3$ will be favored over precipitation and coccolithophores may be less successful in exporting carbon to the deep [*Fabry et al.*, 2008]. Many previous calcification-$CO_2$ response studies investigating potential impacts of ocean acidification (OA) suggest that elevated $CO_2$ reduces organism calcification [*Riebesell et al.*, 2000; *Langer et al.*, 2009; *Zondervan et al.*, 2001; *Delille et al.*, 2005; *Engel et al.*, 2005].

The Southern Ocean (>30°S) absorbs a large fraction of anthropogenic carbon dioxide emissions from the atmosphere [*Sabine et al.*, 2004; *Khatiwala et al.*, 2009]. As a region characterized by low levels of $\left[CO_3^{2-}\right]$ and a shallow $CaCO_3$ saturation horizon [*Feely et al.*, 2009], we are likely to detect the impacts of OA here earlier than elsewhere in the global ocean [*Fabry et al.*, 2009]. High concentrations of coccolithophore particulate inorganic carbon (PIC) extend from the Antarctic continent northward to ~30°S during austral summer, a characteristic detectable from space and referred to as the Great Calcite Belt [*Balch et al.*, 2011]. While some studies attribute elevated concentrations of satellite-estimated PIC here to other scattering sources, such as microbubbles [*Zhang et al.*, 2002] or noncalcifying organisms in the Ross Sea (e.g., *Phaeocystis antarctica*) [*Arrigo et al.*, 1999], many studies support high-coccolithophore abundance in the Great Calcite Belt [*Painter et al.*, 2010; *Balch et al.*, 2011, 2014; *Sadeghi et al.*, 2012]. The Patagonian Shelf, the highest reflectance region within the Belt, is also a highly productive region (Figure S1a in the supporting information) due to upwelling, mixing, tides, and riverine input and home to large coccolithophore blooms in summer [*Painter et al.*, 2010; *Balch et al.*, 2014]. High calcification rates have been estimated within these high-PIC regions [*Balch et al.*, 2007], but changes in these rates have not yet been quantified. Here we present a first estimate of changing calcification rates within the Southern Ocean over the satellite record.

## 2. Methods

This study focuses on austral summer (December, January, and February (DJF)) calcification south of 30°S from 1998 to 2014. We used satellite observations of monthly binned PIC and chlorophyll (CHL)

concentration and sea surface temperature (SST) to calculate calcification rates (C) using equation (1) of *Balch et al.* [2007]:

$$C = 0.2694^{-1}[(-0.0063Z + 0.05081\mathrm{PIC} - 0.01055\mathrm{CHL} + 0.05806D - 0.0079\mathrm{SST}) - 0.4008], \quad (1)$$

where depth ($Z$) is 1 m and daylength ($D$; hours) is calculated for the 15th day of each month as a function of latitude; Sea-viewing Wide Field-of-view Sensor (SeaWiFS) level 3 PIC and chlorophyll (1997–2009) and Advanced Very High Resolution Radiometer (AVHRR) Oceans Pathfinder SST (1997–2009) and Moderate Resolution Imaging Spectroradiometer (MODIS)-Aqua PIC, chlorophyll and SST (2002-2014; both day and night temperature retrievals were equally weighted to maximize data availability) on a 9 km grid. December, January, and February calcification rates of each year were averaged to form a mean summer calcification rate (90 day temporal bins; e.g., December 2002 and January and February 2003 represent *summer 2003*). The RMS error in calcification rate (RMS = ±0.021 mg PIC $m^{-3}$ $d^{-1}$) was derived using the $n^{-0.5}$ technique described in *Balch et al.* [2007]. Since the RMS error is an order of magnitude smaller than the uncertainty in the trend estimates, we report 95% confidence estimates. One continuous record of calcification from 1998 to 2014 was generated at each Southern Ocean location following the regression technique of *Brown and Arrigo* [2012]: we applied linear regression over the 2003–2007 SeaWiFS/MODIS overlap period, excluding 2008–2009 for which limited SeaWiFS data are available, in order to predict calcification from summer 2008 to 2014 (Figure S2).

Calcification rate, PIC, chlorophyll, and SST data were masked for the presence of summer sea ice. We regridded monthly (1998–2012), 25 km sea ice concentrations from Nimbus-7 Scanning Multichannel Microwave Radiometer and DMSP Special Sensor Microwave/Imager-Special Sensor Microwave Imager/Sounder Passive Microwave Data [*Cavalieri et al.*, 1996, updated yearly] to a 9 km grid, using climatological sea ice concentration for missing data points. These data were masked where at least 40 (out of 48) months included some percentage of ice.

Percent changes reported here were determined by (1) calculating the area-weighted mean of a particular location (entire basin or specific region) to create a time series of summers 1998 to 2014, (2) performing linear regression on the time series (in a least squares sense) to find the slope of the fitted line, and (3) multiplying that slope by the length of the time series and dividing by the arithmetic mean of the time series. Basin-wide calculations exclude locations where the summer mean is missing at least 1 month of data.

Carbonate ion concentrations were estimated using the program developed for $CO_2$ system calculations (CO2SYS) [*Lewis and Wallace*, 1998], with the preferred dissociation constants [*Takahashi et al.*, 1982; *Dickson*, 1990; *Uppstrom*, 1979]. Significant trends, in a least squares sense, were found if three or more summer data points existed in the time series at each location. The variables used in the program for the surface (depth) analysis include $fCO_2$ and $pCO_2$ (total $CO_2$ concentration), alkalinity, silicate and phosphate concentration, salinity, SST (temperature), and pressure (see Table S1).

To calculate a change in calcification due to a change in a particular satellite variable, for example, PIC, we find the equation of the line that best fits PIC in a least squares sense. Using the calcification algorithm [*Balch et al.*, 2007], the mean calcification rate at time 1 ($C_i$; year 1998) is calculated as in equation (1), where PIC is the fitted 1998 value. We calculate the estimated final mean rate at time 17 ($C_f$; year 2014) as in equation (1), where PIC is the fitted 2014 value and chlorophyll and SST are held constant at their initial fitted 1998 values. The difference in $C_i$ and $C_f$ is the resulting estimated change in calcification rate due to the change in PIC concentration for a given region.

The location of the Antarctic Polar Front was found using weekly satellite-estimated (Advanced Microwave Scanning Radiometer–EOS (AMSR-E)) sea surface temperature [*Dong et al.*, 2006] from 2002 to 2011 and defined as the absolute SST gradient at each grid point: $[(dT/dx)^2 + (dT/dy)^2]^{1/2}$. Large gradients found near Antarctica were removed. At each longitude, the position is the southernmost location where the SST gradient exceeded 1.5°C per 100 km. Small patches of high SST gradients spanning less than 4° longitude were removed (possible eddy/ring detection) and relaxations of the SST gradient limit were made for large deviations from the temporal mean. See *Dong et al.* [2006] for further detail.

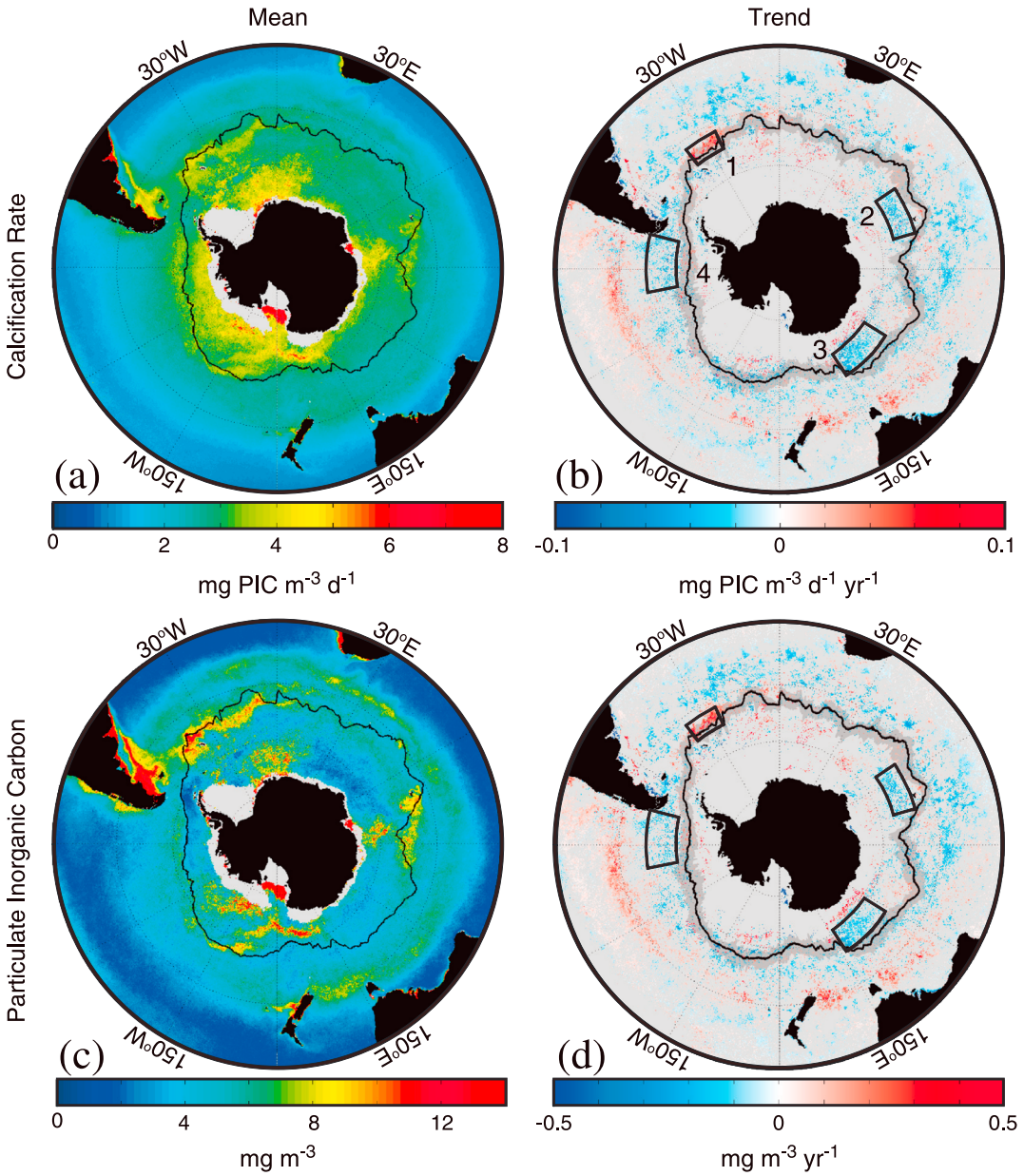


**Figure 1.** Maps of Southern Ocean (>30°S) summer (DJF) mean state of (a) calcification rate and (c) particulate inorganic carbon concentration and linear trends in (b) calcification and (d) PIC, masked for the presence of summer sea ice (see section 2). Only those trends with significance ≥95% are shown. The black line and gray shading indicate the average summer location of the Antarctic Polar Front (see section 2). Boxes indicate regions singled out for further analysis in the (1) Atlantic, (2) western Indian, (3) eastern Indian, and (4) Pacific sectors.

## 3. Results and Discussion

Figure 1a shows the mean rate of summer calcification. We observe a basin-wide average of 2.28 ± 0.021 mg PIC $m^{-3}$ $d^{-1}$, with values lowest in the subtropics and highest south of the Antarctic Polar Front (PF) (Figure 1a). In agreement with previous studies [*Balch et al.*, 2007; *Beaufort et al.*, 2011], we find elevated calcification rates near the Patagonian Shelf and in the vicinity of the Antarctic Circumpolar Current (ACC). Suspended calcite in the Southern Ocean exists at an average concentration of ~4.65 mg $m^{-3}$. A sharp decrease in PIC south of the PF is observed in the Bellingshausen and Amundsen sector (Figure 1c), in agreement with the same gradient reported for coccolithophore abundance in this region [*Gravalosa et al.*, 2008]. We assess the sensitivity of basin-scale calcification rate trends to interannual variability by

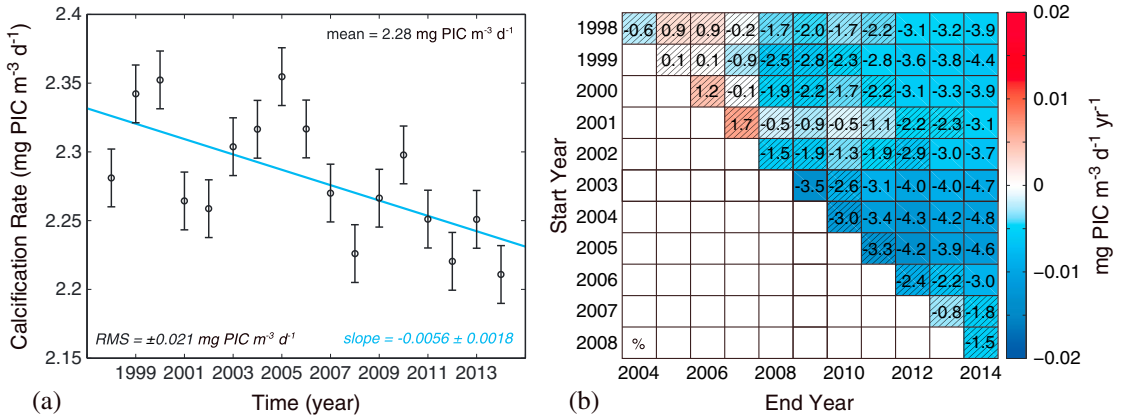


**Figure 2.** (a) Time series of basin area-weighted mean calcification rate from summers 1998 to 2014. Error bars (black) showing expected standard error (with respect to equation (1); see section 2) and fitted least squares line (cyan) provided. (b) Multidecadal trends in basin-mean calcification rate over the same time period. Color bar indicates the slope of the fitted trend line (in units of mg PIC $m^{-3}$ $d^{-1}$ $yr^{-1}$) for each start and end year pair and text shows the percent change in calcification rate with respect to the mean. Trends that are not significant at the 95% level are hatched.

calculating trends for a range of start and end years. The sign of the trends are robust across many start and end year pairs (Figure 2b), suggesting that long-term trends in Southern Ocean calcification are independent of interannual variability.

From 1998 to 2014 we observe a 3.9 ± 1.3% basin-wide reduction in summer calcification (Figure 2a). Throughout the Southern Ocean, significant trends (at the 95% level) in both calcification and PIC are spatially heterogeneous yet negative nearly everywhere in the Atlantic, Indian, and southernmost Pacific sectors (Figures 1b and 1d). Patches of positive trends are found near the PF in the Atlantic sector and near the Subtropical Front in the Pacific sector. We identify four large regions ($\sim 1 \times 10^6$ $km^2$) with significant trends located in the ACC region for further analysis (Figure 1b). Region 1 in the Atlantic shows a 14.3 ± 5.1% (31.3%) increase in calcification rate (PIC concentration) over 1998 to 2014, while Regions 2–4 in the Indian and Pacific sectors have experienced a 9.2 ± 4.4% (20.1%), 11.6 ± 3.1% (34.3%), and 7.5 ± 3.1% (16.8%) decline over this period, respectively (Table 1). We assess the sensitivity of regional calcification rate and PIC trends to interannual variability as above. Again, the sign of the trends are robust across many start and end year pairs (Figure S3), suggesting that long-term trends are independent of interannual variability in these regions. Maps of the mean state and trends of chlorophyll and sea surface temperature are shown in Figure S1.

In order to better understand the role of PIC, chlorophyll, and SST in driving calcification trends, we calculate the contribution of each of these quantities to the total change in calcification rate from 1998 to 2014 in each region (see section 2). Table 1 shows the total change in calcification rate by region and the contribution to the total change from the change in PIC, chlorophyll, and SST over this period; it is clear that the PIC contribution is largest. We conclude that the calcification trends in these regions are primarily driven by changes in PIC concentration.

We investigate the drivers of heterogeneity in Southern Ocean calcification trends by quantifying trends in surface ocean carbonate ion concentration from hydrography data. While the calcification-$CO_2$ response is not completely understood [*Riebesell et al.*, 2000; *Beaufort et al.*, 2011; *Iglesias-Rodriguez et al.*, 2011; *Beaufort et al.*, 2008], we generally expect areas exhibiting negative trends in $[CO_3^{2-}]$ to correspond to areas with decreases in calcification over the satellite period. We used underway surface water fugacity of $CO_2$ ($fCO_2$) and partial pressure of $CO_2$ ($pCO_2$) measurements, together with a combination of concurrent measurements and climatologies of temperature, salinity, alkalinity, silicate, and phosphate to estimate the surface ocean carbonate ion concentration and its change over time [*Lewis and Wallace*, 1998] (see Table S1). The sign of the trends in surface carbonate (Figure 3a) track the sign of the trends in calcification (Figure 1b) and PIC (Figure 1d), particularly in Regions 2 and 3 of the Indian sector where hydrographic data are plentiful. Here a decrease in calcification rate corresponds to a decrease in $[CO_3^{2-}]$ over the satellite period. The remaining two focus regions lack underway data for direct comparison. The Drake Passage, adjacent to

**Table 1.** What Drives Calcification Trends (1998–2014)?

| | Region 1 | Region 2 | Region 3 | Region 4 |
|---|---|---|---|---|
| | *Mean Calcification Rate (mg PIC $m^{-3}$ $d^{-1}$)* | | | |
| | 3.193 | 2.938 | 2.758 | 2.775 |
| | *Changes in calcification (mg PIC $m^{-3}$ $d^{-1}$)* | | | |
| Total change[a] | 0.457 ± 0.164 | −0.269 ± 0.127 | −0.321 ± 0.086 | −0.207 ± 0.086 |
| PIC contribution[b] | 0.483 | -0.227 | -0.271 | -0.155 |
| Chl contribution[b] | -0.007 | 0.002 | 0.002 | 0.001[c] |
| SST contribution[b] | -0.009[c] | -0.008[c] | -0.017[c] | -0.002[c] |
| | *Mean PIC (mg $m^{-3}$)* | | | |
| | 8.169 | 5.967 | 4.179 | 4.893 |
| | *Changes in PIC (mg $m^{-3}$)* | | | |
| | 2.560 ± 0.909 | −1.201 ± 0.648 | −1.434 ± 0.452 | −0.823 ± 0.425 |

[a]95% confidence interval reported for total change because RMS error is an order of magnitude smaller.
[b]Sum of contributions ≠ total change values exactly (see section 2).
[c]Trends used in calculation not statistically significant at ≥95% level.

our Region 4, has seen a decrease in summer [$CO_3^{2-}$] (D. R. Munro et al., Recent evidence for a strengthening $CO_2$ sink in the Southern Ocean from $pCO_2$ measurements in the Drake Passage (2002–2014), *Geophysical Research Letters,* in review, 2015). Given the relatively fast transport in this region of the Southern Ocean, the Drake Passage signal of decreasing [$CO_3^{2-}$] could possibly be identified in Region 4 where we observe a significant decrease in calcification.

We estimated changes in the upper water column carbonate ion concentration from bottle data collected on transect SR03, on the eastern edge of our Region 3 (Figure 3b). Although hydrographic data from this line are relatively sparse in time, it is the only location with enough carbonate chemistry data to calculate full depth trends in any of our four regions. Our analysis of this data indicates that the upper 200 m south of the PF have experienced a significant decrease in carbonate over 1994–2003. *Cubillos et al.* [2007] observed a north-south decline in calcification within the Australian sector over summers 2003 to 2006; they attribute this decline to shifts in calcifier morphotype abundance and distribution rather than changes in carbonate chemistry or surface warming. Here we show that in addition to any shifts in interspecies dominance occurring over the past two decades, changes in carbonate chemistry (Figure 3) and surface warming (Figure S1d) are concurrent with changes in calcification rates in this sector. Overall, our carbonate analyses

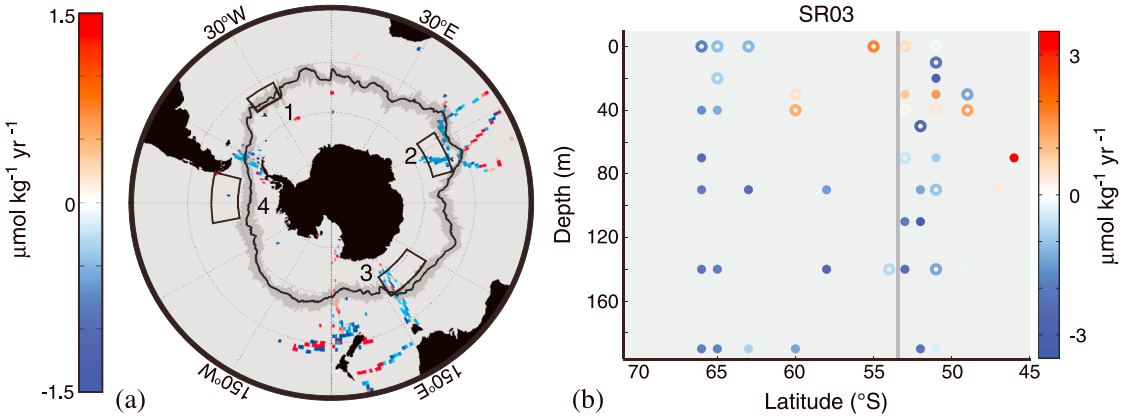


**Figure 3.** (a) Significant trends (at the 95% level) in summer surface carbonate from continuous underway $fCO_2$ (1998–2011) and $pCO_2$ (1998–2013); the trends using these carbon parameters were calculated separately and then overlaid on the same plot. (b) All trends in the zonal mean carbonate ion concentration at depth from bottle data along repeat transect SR03 in our Region 3 (1994, 1996, 1998, 2001, and 2003), where filled circles indicate significance at the 95% level and open circles, otherwise. Mean position of Antarctic Polar Front indicated by the (Figure 3a) black line and (Figure 3b) gray line. See Table S1 for data information.

suggest that the observed regional decreases in calcification correspond to regions exhibiting decreases in carbonate over similar time periods.

The proximity of these four focus regions to the Antarctic Polar Front begs the question whether there exists any association between variability in the location of the front and the observed calcification trends. In order to assess the variability in frontal position over time, we adapted and extended the PF analysis performed by *Dong et al.* [2006] by calculating the PF location from all available weekly AMSR-E satellite SST data (2002–2011; see section 2). The austral summer mean PF location is plotted as the black line in Figures 1 and 3 while the darker gray shaded area surrounding the mean (Figures 1b, 1d, and 3a) indicates the minimum and maximum latitudinal extent of the PF at any given time. The majority of trends observed (Figures 1b and 1d) are unrelated to variation in frontal location, with the exception of the positive trends observed in Region 1; the same is true for trends in chlorophyll concentration (Figure S1b).

We find a significant southward shift in the mean position of the PF from summers 2003 to 2011 in Region 1 (Figure S4). This poleward shift may have altered the physical and chemical properties of seawater in this region over time, particularly those that influence interspecies competition for available nutrients. Previous research indicates that the PF marks the boundary between silicate-poor and silicate-rich waters [*Sarmiento et al.*, 2004]. Diatoms, the dominant plankton in the Southern Ocean, require a sufficient amount of silicic acid for production. A southward migration of the PF over this 9 year period may have reduced the availability of surface silicic acid here and therefore the ability of diatoms to effectively compete for nutrients. Such a change may have allowed coccolithophores to become more dominant in this region. One possible explanation for the positive trends in calcification (Figure 1b) and PIC (Figure 1d) in Region 1 is this southward migration of the PF over time.

Calculating trends in calcification rates from satellite observations comes with several caveats. The calcification algorithm used here, while validated, published, and widely used, was empirically derived from observations made primarily in the Northern Hemisphere oceans [*Balch et al.*, 2007]. A more complete picture of changing calcification rates in the Southern Ocean from satellite products requires additional observations and validation using data collected in this region. Previous studies have suggested that chlorophyll concentration is underestimated in the Southern Ocean [*Johnson et al.*, 2013]. Other studies find large underestimates in mean PIC from satellite; *Beaufort et al.* [2008] report the greatest density of coccoliths (individual calcite plates) at a depth below what is deemed detectable via satellite. However, it has also been suggested that PIC is being largely overestimated in the Southern Ocean (R. Johnson, manuscript in preparation, 2015). Figure S5 demonstrates that overestimations/underestimations in PIC or chlorophyll concentration do not affect the trends reported here. The estimates presented here represent calcification and PIC standing stock occurring in the topmost layer of the ocean and are therefore not representative of these variables throughout the rest of the sunlit layer. Regardless of potential biases in the mean rate of calcification estimated from satellite, the variability and trends in both calcification rate and PIC concentration reported here are statistically robust.

## 4. Conclusions

In summary, we demonstrate that surface calcification and PIC concentrations have decreased in large portions of the Southern Ocean over the satellite record, concurrent with significant decreases in the surface ocean carbonate ion concentration. One exception is a large region of the Atlantic sector where positive trends in calcification rate correspond to a southward shift of the PF. In addition to changing carbonate chemistry as a result of global change, coccolithophores and other calcifiers will also experience increased stress from other physical and chemical factors that will likely impact organism processes. These results suggest that large-scale shifts in the ocean carbon cycle are already occurring and highlight organism and marine ecosystem vulnerability in a changing climate.

**Acknowledgments**

The SeaWiFS and MODIS-Aqua level 3 particulate inorganic carbon, chlorophyll-*a* and sea surface temperature data were obtained from the NASA Ocean Colour distributed archive (http://oceancolor.gsfc.nasa.gov/). The AVHRR Oceans Pathfinder sea surface temperature data used in conjunction for the SeaWiFS era were obtained from http://www.science.oregonstate.edu/ocean.productivity/ and regridded to a 9 km grid. CO2SYS is obtainable from cdiac.ornl.gov/oceans/co2rprt.html. Weekly SST observations from AMSR-E ocean products used for the polar front analysis obtained online at http://www.ssmi.com. We acknowledge generous funding from NSF (DGE-1144083 and OCE-1155240) and NOAA (NA12OAR4310058). We thank Shenfu Dong for her help and guidance in our effort to extend the Polar Front analysis.

The Editor thanks one anonymous reviewer for assisting in the evaluation of this paper.

## References

Arrigo, K. R., D. H. Robinson, D. L. Worthen, R. B. Dunbar, G. R. DiTullio, M. VanWoert, and M. P. Lizotte (1999), Phytoplankton community structure and the drawdown of nutrients and $CO_2$ in the Southern Ocean, *Science*, *283*, 365–367, doi:10.1126/science.283.5400.365.

Balch, W. M., D. Drapeau, B. Bowler, and E. Booth (2007), Prediction of pelagic calcification rates using satellite measurements, *Deep Sea Res., Part II*, *54*(5-7), 478–495, doi:10.1016/j.dsr2.2006.12.006.

Balch, W. M., D. T. Drapeau, B. C. Bowler, E. Lyczskowski, E. S. Booth, and D. Alley (2011), The contribution of coccolithophores to the optical and inorganic carbon budgets during the Southern Ocean Gas Exchange Experiment: New evidence in support of the Great Calcite Belt hypothesis, *J. Geophys. Res.*, *116*, C00F06, doi:10.1029/2011JC006941.

Balch, W. M., D. T. Drapeau, B. C. Bowler, E. R. Lyczkowski, L. C. Lubelczyk, S. C. Painter, and A. J. Poulton (2014), Surface biological, chemical, and optical properties of the Patagonian Shelf coccolithophore bloom, the brightest waters of the Great Calcite Belt, *Limnol. Oceanogr.*, *59*(5), 1715–1732, doi:10.4319/lo.2014.59.5.1715.

Beaufort, L., M. Couapel, N. Buchet, H. Claustre, and C. Goyet (2008), Calcite production by coccolithophores in the south east Pacific Ocean, *Biogeosciences*, *5*, 1101–1117, doi:10.5194/bg-5-1101-2008.

Beaufort, L., et al. (2011), Sensitivity of coccolithophores to carbonate chemistry and ocean acidification, *Nature*, *476*(7358), 80–83, doi:10.1038/nature10295.

Brown, Z. W., and K. R. Arrigo (2012), Contrasting trends in sea ice and primary production in the Bering Sea and Arctic Ocean, *ICES J. Mar. Sci.*, *69*, 1180–1193, doi:10.1093/icesjms/fss113.

Cavalieri, D. J., C. L. Parkinson, P. Gloersen, and H. Zwally (1996, updated yearly), *Sea Ice Concentrations From Nimbus-7 SSMR and DMSP SSM/I-SSMIS Passive Microwave Data*, NASA National Snow and Ice Data Center Distributed Active Archive Center, Boulder, Colo.

Cubillos, J. C., S. W. Wright, G. Nash, M. de Salas, B. Griffiths, B. Tilbrook, A. Poisson, and G. M. Hallegraeff (2007), Calcification morphotypes of the coccolithophorid *Emiliania huxleyi* in the Southern Ocean: Changes in 2001 to 2006 compared to historical data, *Mar. Ecol. Prog. Ser.*, *348*, 47–54, doi:10.3354/meps07058.

Delille, B., et al. (2005), Response of primary production and calcification to changes of $pCO_2$ during experimental blooms of the coccolithophorid *Emiliania huxleyi*, *Global Biogeochem. Cycles*, *19*, GB2023, doi:10.1029/2004GB002318.

Dickson, A. G. (1990), Standard potential of the reaction: AgCl(s) + 1/2 $H_2$(g) = Ag(s) + HCl(aq), and the standard acidity constant of the ion $HSO_4^-$ in synthetic seawater from 273.15 to 318.15 K, *J. Chem. Thermodyn.*, *22*, 113–127.

Dong, S., J. Sprintall, and S. T. Gille (2006), Location of the Antarctic polar front from AMSR-E satellite sea surface temperature measurements, *J. Phys. Oceanogr.*, *36*, 2075–2089, doi:10.1175/JPO2973.1.

Engel, A., I. Zondervan, K. Aerts, L. Beaufort, A. Benthien, L. Chou, B. Delille, J. P. Gattuso, J. Harlay, and C. Heemann (2005), Testing the direct effect of $CO_2$ concentration on a bloom of the coccolithophorid *Emiliania huxleyi* in mesocosm experiments, *Limnol. Oceanogr.*, *50*, 493–507, doi:10.4319/lo.2005.50.2.0493.

Fabry, V. J., B. A. Seibel, R. A. Feely, and J. C. Orr (2008), Impacts of ocean acidification on marine fauna and ecosystem processes, *ICES J. Mar. Sci.*, *65*, 414–432.

Fabry, V. J., J. B. McClintock, J. T. Mathis, and J. M. Grebmeier (2009), Ocean acidification at high latitudes: The bellwether, *Oceanography*, *22*(4), 160–171.

Feely, R. A., S. C. Doney, and S. R. Cooley (2009), Ocean acidification: Present conditions and future changes in a high-$CO_2$ world, *Oceanography*, *22*(4), 36–47.

Gravalosa, J. M., J.-A. Flores, F. J. Sierro, and R. Gersonde (2008), Sea surface distribution of coccolithophores in the eastern Pacific sector of the Southern Ocean (Bellingshausen and Amundsen Seas) during the late austral summer of 2001, *Mar. Micropaleontol.*, *69*(1), 16–25, doi:10.1016/j.marmicro.2007.11.006.

Iglesias-Rodriguez, M. D., et al. (2008), Phytoplankton calcification in a high-$CO_2$ world, *Science*, *320*(5874), 336–340, doi:10.1126/science.1154122.

Johnson, R., P. G. Strutton, S. W. Wright, A. McMinn, and K. M. Meiners (2013), Three improved satellite chlorophyll algorithms for the Southern Ocean, *J. Geophys. Res. Oceans*, *118*, 3694–3703, doi:10.1002/jgrc.20270.

Khatiwala, S., F. Primeau, and T. Hall (2009), Reconstruction of the history of anthropogenic $CO_2$ concentrations in the ocean, *Nature*, *462*, 346–349, doi:10.1038/nature08526.

Langer, G., G. Nehrke, I. Probert, J. Ly, and P. Ziveri (2009), Strain-specific responses of *Emiliania huxleyi* to changing seawater carbonate chemistry, *Biogeosci. Discuss.*, *6*(2), 4361–4383, doi:10.5194/bgd-6-4361-2009.

Lewis, E., and D. W. R. Wallace (1998), Program developed for $CO_2$ system calculations, *ORNL/CDIAC-105*, Carbon Dioxide Inf. Anal. Cent. (CDIAC), Oak Ridge Natl. Lab., U.S. Dep. of Energy, Oak Ridge, Tenn.

Painter, S. C., A. J. Poulton, J. T. Allen, R. Pidcock, and W. M. Balch (2010), The COPAS'08 expedition to the Patagonian Shelf: Physical and environmental conditions during the 2008 coccolithophore bloom, *Cont. Shelf Res.*, *30*, 1907–1923, doi:10.1016/j.csr.2010.08.013.

Riebesell, U., I. Zondervan, B. Rost, P. D. Tortell, R. E. Zeebe, and F. M. M. Morel (2000), Reduced calcification of marine plankton in response to increased atmospheric $CO_2$, *Nature*, *407*, 364–367.

Sabine, C. L., et al. (2004), The oceanic sink for anthropogenic $CO_2$, *Science*, *305*(5682), 367–371, doi:10.1126/science.1097403.

Sadeghi, A., T. Dinter, M. Vountas, B. Taylor, M. Altenburg-Soppa, and A. Bracher (2012), Remote sensing of coccolithophore blooms in selected oceanic regions using the PhytoDOAS method applied to hyper-spectral satellite data, *Biogeosciences*, *9*, 2127–2143, doi:10.5194/bg-9-2127-2012.

Sarmiento, J. L., N. Gruber, M. A. Brzezinski, and J. P. Dunne (2004), High-latitude controls of thermocline nutrients and low latitude biological productivity, *Nature*, *427*, 56–60, doi:10.1038/nature02204.1.

Takahashi, T., R. T. Williams, and D. L. Bos (1982), Carbonate chemistry, in *GEOSECS Pacific Expedition, Volume 3, Hydrographic Data 1973-1974*, edited by W. S. Broecker, D. W. Spencer, and H. Craig, pp. 77–83, National Science Foundation, Washington, D. C.

Uppstrom, L. R. (1979), The boron/chloronity ratio to deep-sea water from the Pacific Ocean, *Deep Sea Res.*, *21*, 161–162.

Zhang, Z., M. Lewis, M. Lee, B. Johnson, and G. Korotaev (2002), The volume scattering function of natural bubble population, *Limnol. Oceanogr.*, *47*(5), 1273–1282.

Zondervan, I., R. E. Zeebe, B. Rost, and U. Riebesell (2001), Decreasing marine biogenic calcification: A negative feedback on rising atmospheric $pCO_2$, *Global Biogeochem. Cycles*, *15*, 507–516, doi:10.1029/2000GB001291.